Journal of Hazardous Materials 189 (2011) 465–471

Contents lists available at ScienceDirect

Journal of Hazardous Materials

journal homepage: www.elsevier.com/locate/jhazmat

Photocatalytic and antibacterial properties of a TiO_2/nylon-6 electrospun nanocomposite mat containing silver nanoparticles

Hem Raj Pant[a,b], Dipendra Raj Pandeya[c], Ki Taek Nam[d], Woo-il Baek[d], Seong Tshool Hong[c], Hak Yong Kim[d,*]

[a] Department of Bionanosystem Engineering, Chonbuk National University, Jeonju 561-756, Republic of Korea
[b] Department of Engineering Science and Humanities, Institute of Engineering, Pulchowk Campus, Tribhuvan University, Kathmandu, Nepal
[c] Department of Microbiology and Immunology, Institute for Medical Science, Chonbuk National University, Jeonju, 561-756, Republic of Korea
[d] Department of Textile Engineering, Chonbuk National University, Jeonju 561-756, Republic of Korea

ARTICLE INFO

Article history:
Received 21 January 2011
Received in revised form 17 February 2011
Accepted 17 February 2011
Available online 24 February 2011

Keywords:
Electrospinning
Spider-wave
Antimicrobial
TiO_2/nylon-6
Ag nanoparticles

ABSTRACT

Silver-impregnated TiO_2/nylon-6 nanocomposite mats exhibit excellent characteristics as a filter media with good photocatalytic and antibacterial properties and durability for repeated use. Silver nanoparticles (NPs) were successfully embedded in electrospun TiO_2/nylon-6 composite nanofibers through the photocatalytic reduction of silver nitrate solution under UV-light irradiation. TiO_2 NPs present in nylon-6 solution were able to cause the formation of a high aspect ratio spider-wave-like structure during electrospinning and facilitated the UV photoreduction of $AgNO_3$ to Ag. TEM images, UV–visible and XRD spectra confirmed that monodisperse Ag NPs (approximately 4 nm in size) were deposited selectively upon the TiO_2 NPs of the prepared nanocomposite mat. The antibacterial property of a TiO_2/nylon-6 composite mat loaded with Ag NPs was tested against *Escherichia coli*, and the photoactive property was tested against methylene blue. All of the results showed that TiO_2/nylon-6 nanocomposite mats loaded with Ag NPs are more effective than composite mats without Ag NPs. The prepared material has potential as an economically friendly photocatalyst and water filter media because it allows the NPs to be reused.

1. Introduction

The prevention of toxic chemical and microbial contamination is essential in the health care system. Therefore, the development of effective material having both photocatalytic and antimicrobial properties is of great significance. Many studies show that TiO_2 NPs can be widely applied in environmental remediation because of their availability, nontoxicity, stability, low cost and efficiency [1]. The commercially available TiO_2 (Degussa, P-25), an ultra-fine catalysts with a sub-nanometer size, presents superior chemical activity due to the large surface-to-volume ratios. However, in a large scale photocatalytic process, separating powder photocatalysts from solution after the reaction is difficult, and the tendency of the NPs to agglomerate into larger particles will result in a reduction of the photocatalytic efficiency during the cycling use [2]. Furthermore, free TiO_2 NPs present in the environment have been shown to be harmful to living organisms [3]. Another drawback of TiO_2 NPs, used as photocatalyst, is their wide band gap (≈3.2 eV) which is only effective under UV radiation [4]. The deposition of noble metals, such as Ag, Au, Pt, Ru, Rh, and Pd, onto TiO_2 can effectively improve the photocatalytic activity of TiO_2, even in the absence of UV radiation [5–7]. It is achieved due to the electron transfer from TiO_2 to metal NPs, which decreases the number of electron-hole recombination events. Among the noble metal/TiO_2 photocatalysts, Ag/TiO_2 composite materials have attracted particular attention for their low cost and the superior properties of silver [8–13]. It is now well established that the catalytic properties of Ag depend on the dimensions of the supporting material, the preparation method, and particularly, the shape and size of the Ag clusters [6,14].

To prevent the NPs used as photocatalysts from being wasted, some groups have used films or fibers with different polymers containing these nanoparticles [15–21]. However, the aggregation of NPs in solution makes these processes difficult, and the exposed surface area for the appropriate reaction cannot be maintained. Furthermore, the presence of inorganic NPs increases the diameter of the polymeric nanofibers during electrospinning, which decreases the surface-to-volume ratio of the material [19]. The aim of the present work was to create high-aspect-ratio polymeric nanofiber mats for TiO_2 NPs onto which Ag NPs could be decorated without aggregation. Moreover, this process was conducted without any capping or reducing polymeric reagent. In this work, we used TiO_2 NPs as anchoring sites (for Ag NPs), which is incorporated with the polymer matrix by means of electrospinning. Our previous work showed that the electrospinning of a small amount of TiO_2 NPs

* Corresponding author. Tel.: +82 632702351; fax: +82 632704249.
E-mail address: khy@jbnu.ac.kr (H.Y. Kim).

0304-3894/$ – see front matter © 2011 Elsevier B.V. All rights reserved.
doi:10.1016/j.jhazmat.2011.02.062

with nylon-6 can give a spider-wave-like structure [22]. The formation of such spider-wave nanofibers (up to the sub-nanoscale) allows the creation more reactive sites [23]. We expect that well-dispersed TiO_2 NPs on these high aspect ratio spider-wave-like nanofibers can provide more surface area for the photocatalytic deposition of Ag NPs without aggregation from the $AgNO_3$ solution upon UV-radiation exposure. The development of this type of effective photocatalysts may be considered a breakthrough in industrial-scale utilization of solar energy to address environmental needs.

Nylon-6 is a synthetic polymeric material that is widely used in many industrial fields because of its low cost, superior fiber forming ability, good mechanical strength, and strong chemical and thermal stability [24,25]. Hence, the nanocomposite material obtained from nylon-6, TiO_2 and Ag is a potential candidate for many different applications. The resulting silver-coated TiO_2 on the nylon-6 nanofiber showed not only the effective photocatalytic activity in the oxidation of dyes but also showed good bactericidal effects in water even in the absence of UV radiation. Hence, this (cost effective) nanocomposite material will be a potential water filter media for people in developing countries, where millions of people die each year due to contaminated drinking water.

2. Experimental procedure

2.1. Preparation of nylon-6/TiO_2 nanocomposite mat

A nylon-6/TiO_2 nanocomposite mat was prepared by mixing 1 wt% of TiO_2 NPs (Aeroxide P25, 80% anatase, 20% rutile, with an average particle size of 21 nm and a specific surface area of $50 \pm 15\ m^2\ g^{-1}$) with a 20 wt% nylon-6 (KN20 grade, Kolon, Korea) solution prepared in a 4:1 ratio by weight of formic acid and acetic acid (Showa, Japan). The electrospinning process was carried out with a voltage of 18 kV and 18 cm from the collector to the tip of the syringe. After vacuum drying for 24 h, the fiber mat was used for further analysis.

2.2. Silver photodeposition on the TiO_2/nylon-6 nanocomposite mat

For silver photodeposition, nylon-6 and TiO_2/nylon-6 nanocomposite matrices (4 cm × 4 cm) were placed into 5 ml of 1×10^{-4} M $AgNO_3$ solution. The photodeposition was conducted under UV light (at 254 nm) for irradiation times of 15, 30 and 60 s, respectively. After washing with distilled water, the mats were vacuum dried for 24 h at room temperature.

2.3. Characterization

The surface morphology of the nanofibers was studied by field-emission scanning electron microscopy (FE-SEM, S-7400, Hitachi, Japan). The EDX spectrum of a Ag–TiO_2/nylon-6 nanocomposite mat was also recorded with the same FE-SEM instrument. Information about the phase and crystallinity was obtained with a Rigaku X-ray diffractometer (XRD, Rigaku, Japan) with Cu Kα (λ = 1.540 Å) radiation over Bragg angles ranging from 10° to 80°. High resolution images of nanofibers containing TiO_2 NPs were obtained via transmission electron microscopy (TEM, JEM-2010, JEOL, Japan) with a 200 kV accelerating voltage. The samples were prepared either by directly collecting the nanofibers on the TEM grid during electrospinning or by microtome cutting of the nanofibers mats. In addition, TEM EDX (JEM-2200, JEOL, Japan) was used to observe the deposition of the Ag NPs and their sizes on the surface of the TiO_2 NPs. The UV–visible spectra of different nanofiber mats were obtained with a UV–visible spectrometer (Lambda 900, Perkin-Elmer, USA) over the range of 200–800 nm.

2.4. Photocatalytic activity measurements

The photocatalytic activity of different mats was evaluated by observing the degradation of methylene blue (MB) dye solution in a simple photochemical reactor. In the present investigation, the reactions were carried out in Petri dishes of 1.5 cm in height and 5.5 cm in diameter under sunlight. The experiment was conducted in a natural atmospheric environment on a sunny day (between 10 AM and 1 PM) in September (the average amount of solar radiation 16.21 MJ/m^2). For the photodegradation experiments, 25 ml of dye (10 ppm concentration) was reacted with different mats in the Petri dish. The samples were taken at regular intervals of time, and the concentration of the dye was measured by recording its absorbance at 663 nm with a UV–visible spectrophotometer (HP 8453 UV–vis spectroscopy system, Germany).

2.5. Antibacterial property test

The antibacterial activity of different mats was tested against *Escherichia coli* (*E. coli*), which is a waterborne pathogenic microorganism. *E. coli* was cultivated in 100 ml of a Tryptic Soy Broth solution to give a bacterial concentration of about 4.5×10^8 CFU/ml, which was incubated at 37 °C for 12 h with shaking. After washing and centrifugation at 4000 rpm, the *E. coli* bacteria were resuspended and diluted up to several decimal dilutions. Before the nanofiber exposing the bacteria under daylight, the diluted cell solution was incubated at 37 °C for 12 h on a Tryptic Soy Broth solution in dark. The number of viable cells was determined by counting the colonies. For the antibacterial testing, different mats (4 cm × 4 cm in area) were placed into the solution and kept at room condition in day time for 4 h. After this, 0.1 ml of the solution was extracted and quickly spread on Tryptic Soy agar pates. The number of viable *E. coli* cells was determined by plating the extracted solution onto the Tryptic Soy agar plate and counting colonies after 12 h of incubation at 37 °C. The average number of viable cells was obtained by repeating the above procedure three times with error bars.

3. Results and discussion

3.1. Morphology of electrospun mats

The morphologies of electrospun pristine nylon-6 and nylon-6/TiO_2 nanocomposite mats are shown in Fig. 1A and B, respectively. From these images, it is clear that the pristine nylon-6 mat does not contain any spider-wave-like structure whereas the nanocomposite mat with 1% TiO_2 consists of a highly interconnected spider-wave-like structure. The cause and mechanism of the formation of the spider-wave-like structure was explained in our previous work [22]. To support the reported mechanism, we performed a microtome TEM analysis of the 1 wt% TiO_2 nanocomposite mat. Fig, 1D clearly shows that the TiO_2 NPs are well-distributed throughout the spider-wave-like structure of composite mat, which supports the assertion that the TiO_2 NPs are responsible for the formation of the high-aspect-ratio spider-wave-like nanostructure. The good interaction of nylon-6 with TiO_2 NPs may be due to the formation of complex compound of TiO_2 with the C=O group of nylon-6.

We decorated these TiO_2 NPs present on the high-aspect-ratio spider-wave nanofibers with monodispersed Ag NPs by the photocatalytic deposition of Ag NPs from $AgNO_3$ solution in the presence of UV light. The photographs of different mats after the photodeposition of Ag from $AgNO_3$ at different times (Fig. 2) show that the Ag NPs are not deposited on the pure nylon-6 mat because the color of the mat does not change, but the TiO_2/nylon-6 mat becomes

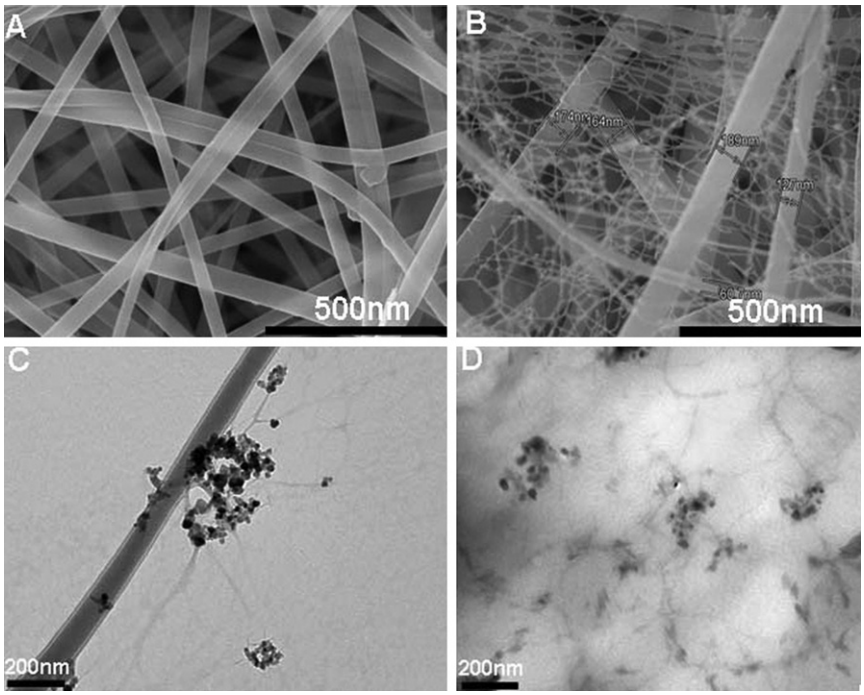

Fig. 1. FSEM images of pristine nylon-6 mat (A) and TiO_2/nylon-6 mat (B). TEM images of TiO_2/nylon-6 nanofibers (C) and microtome TEM of TiO_2/nylon-6 nanofibers (D).

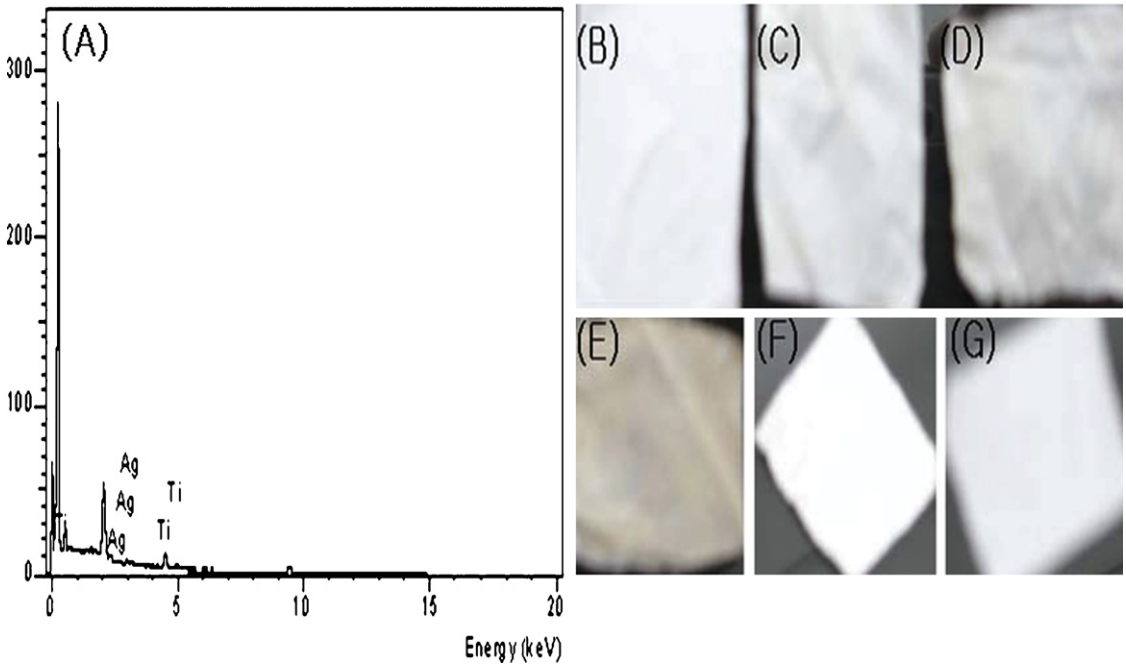

Fig. 2. (A) SEM-EDX of an Ag–TiO_2/nylon-6 mat. (B), (C), (D), and (F) the photographs of the TiO_2/nylon-6 mats after 0, 15, 30 and 60 s UV irradiation in a $AgNO_3$ solution, respectively. (F) and (G) the photographs of pure nylon-6 before and after 60 s UV irradiation in a $AgNO_3$ solution, respectively.

more brownish-gray with the increasing duration of UV irradiation, which shows that the Ag NPs are deposited on it. Longer irradiation times were observed to greatly enhance the photoreduction of the Ag ions and led to the formation of a considerable amount of Ag NPs on the surface of the TiO_2 NPs. Therefore, TiO_2 present on nylon-6 nanofibers not only act as catalyst for the reduction of $AgNO_3$ but also act as anchoring sites for Ag NPs to be attached on the surface of nanofibers.

To investigate the distribution of Ag NPs and their size on the TiO_2/nylon-6 nanofibers, linear analysis TEM EDX was utilized. Fig. 3 shows that both Ag and TiO_2 NPs are present on the polymeric mat. Furthermore, Fig. 3D shows the size of the Ag NPs (approximately 4 nm) deposited on the surface of the TiO_2 NPs. From this image, it is clear that Ag NPs were deposited on the surface of the TiO_2 NPs without aggregation. Silver NPs (≈4 nm) deposited upon the surface of the TiO_2 NPs could greatly accelerate the rate of a photocatalytic reaction by effectively consuming the produced electrons thereby reducing the deleterious recombination of electrons and holes [26]. Under these conditions, the enormous amount of free electrons and holes can be used for the decomposition of

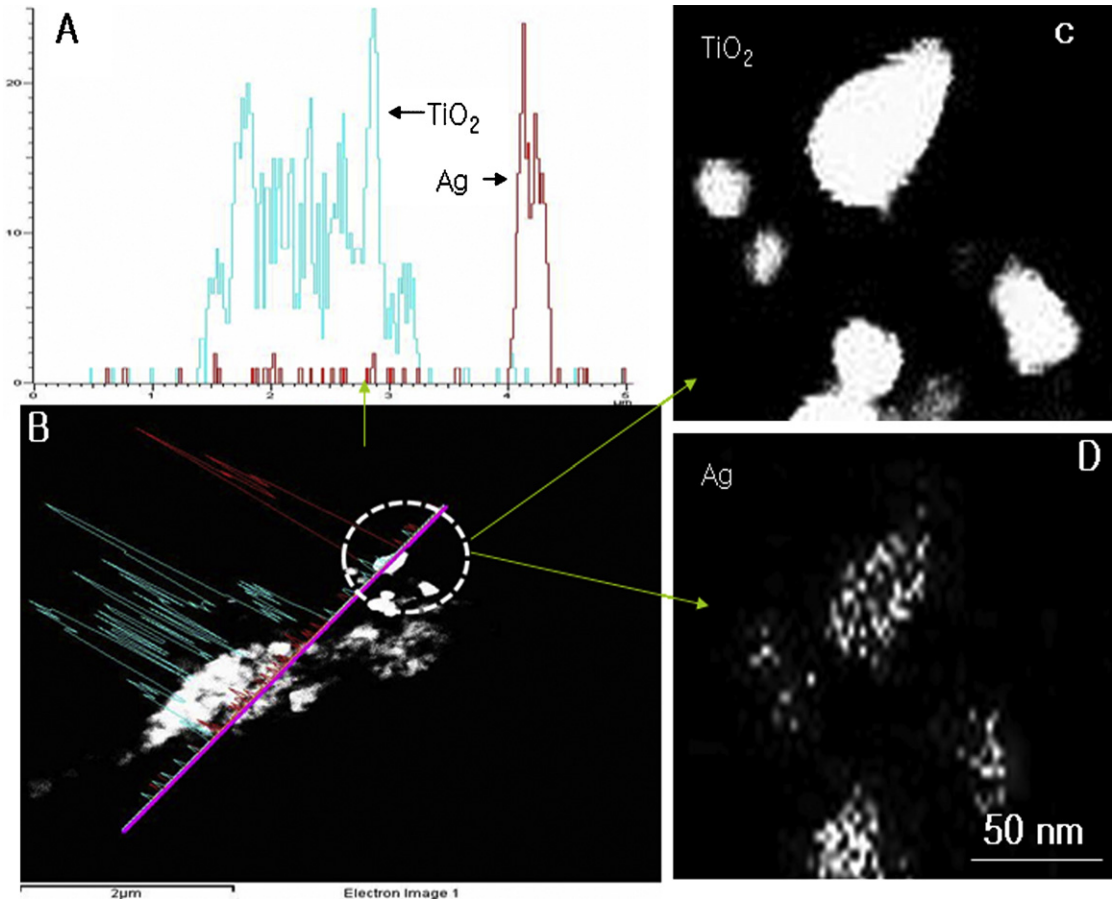

Fig. 3. TEM-EDX of Ag–TiO_2/nylon-6 nanofibers: EDX spectra of TiO_2 and Ag NPs (A), TEM-EDX image of nanocomposite fibers (B), TiO_2 NPs on the nanocomposite mat (C), and Ag NPs on the surface of TiO_2 (D).

organic materials: therefore, the photodegradation and antimicrobial capacities are enhanced as explained in Sections 3.2 and 3.3. Furthermore, this interfacial interaction of Ag–TiO_2 can act as the barrier to the oxidation of metal nanoparticles which can enhance the chemical stability of the Ag NPs.

The deposition of the Ag NPs on the TiO_2 NPs was further confirmed by XRD and UV–visible spectra analyses. The XRD patterns of the nylon-6, TiO_2/nylon-6 and Ag–TiO_2/nylon-6 composite mats are shown in Fig. 4. The XRD patterns of pristine nylon-6 and TiO_2/nylon-6 are explained in our previous work [22]. Comparing the XRD spectra of the TiO_2/nylon-6 and Ag–TiO_2/nylon-6 mats (Fig. 4B and C) shows that the peak at $2\theta = 38$ is broadened and a new peak appears at $2\theta = 44.39$ due to the Ag NPs [27]. The UV–visible measurements (200–800 nm) of different mats are shown in Fig. 5. From the results, the spectrum of TiO_2/nylon-6 indicates that TiO_2 only has no absorption in the spectral region above 420 nm. After the deposition of Ag NPs onto the TiO_2/nylon-6 mat, the absorption curve of Ag–TiO_2/nylon-6 was obviously improved in the 380–780 nm spectral region. This additional absorption peak in the visible region occurs due to the surface plasmon resonance (SPR) effect, which describes the interference of electromagnetic field with the conduction electrons of silver particles dispersed on the TiO_2 NPs. The enhanced absorption is an indication of the greater probability of enhancing the photocatalytic efficiency of Ag–TiO_2 by broadening the light absorption in the visible region with Ag NPs. The fact that the reflection capacity of the Ag–TiO_2/nylon-6 mat is lower than that of the others conforms that the new composite material is better for protective clothing because Ag–TiO_2/nylon-6 can absorb more UV light. The presence of Ag in the electrospun TiO_2/nylon-6 nanocomposite was also confirmed with SEM-EDX, as shown in Fig. 2A.

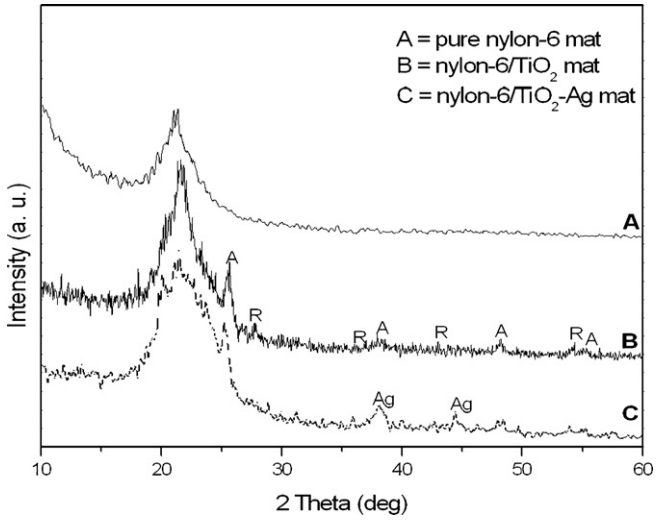

Fig. 4. XRD pattern for pristine nylon-6 (A) TiO_2/nylon-6 (B), and Ag–TiO_2/nylon-6 (C) nanocomposite mats.

3.2. Photodegradation properties of the nanocomposite mats

The photocatalytic performance of the TiO_2/nylon-6 and Ag–TiO_2/nylon-6 composite mats was evaluated by degrading the methylene blue (MB) under solar light irradiation. It has been

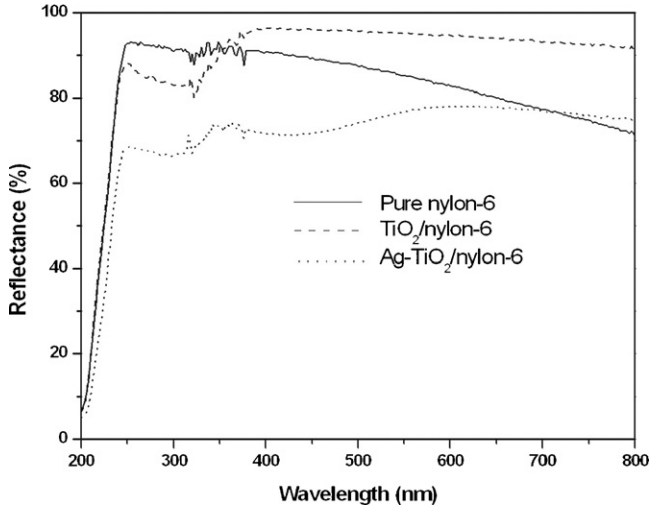

Fig. 5. UV–visible spectra of pure nylon-6 and different nanocomposite mats.

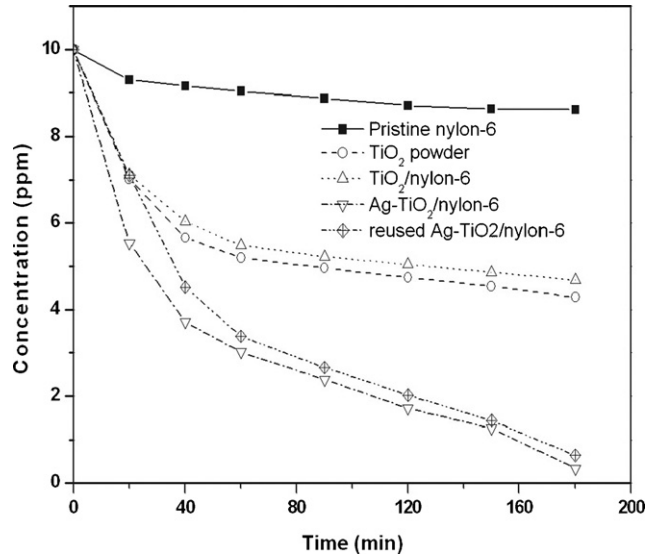

Fig. 6. Comparison of the MB photodegradation in different specimen under sunlight.

reported that MB may decompose itself under UV or solar light irradiation [28]. From Fig. 6, it is clear that the efficiency of the TiO_2/nylon-6 mat is greatly increased by the deposition of Ag nanoparticles. This outcome may occur because of the Ag NPs deposited on the TiO_2/nylon-6 which act as electron traps and enhance the electron–hole separation and the subsequent transfer of trapped electrons to the adsorbed O_2, which acts as an electron acceptor [26]. Furthermore, the higher chemical activity of the Ag-loaded TiO_2/nylon-6 mat can be explained by considering the Ag NPs to form locally Schottky junctions with high potential gradients established by Schottky barrier than at the TiO_2/dye interface. Therefore, efficient charge separation of the light-generated electron–hole pairs can be achieved [29–31]. More effective cause to increase the efficiency of Ag–TiO_2/nylon-6 mat may be due to the surface plasmon resonance of the Ag NPs which is excited by the sunlight and facilitates the excitation of the surface electron and interfacial electron transfer [32]. We compare the relative photocatalytic efficiency of TiO_2 NPs incorporated into the spider-wave fiber and free TiO_2 powder. Approximately the same amount of TiO_2 that was present in mat was weighed and made into a suspension with 25 ml of water. The experiment was carried

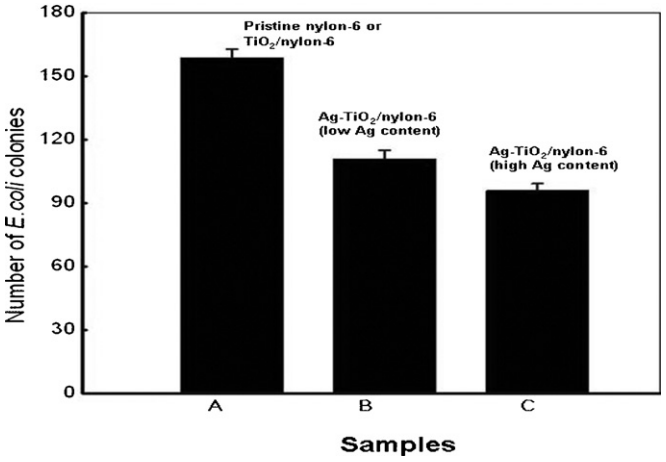

Fig. 7. Number of *E. coli* colonies grown on LB agar plates after treatment with different mats in the daylight for 4 h: (A) pristine nylon-6 or TiO_2/nylon-6 or dark (neither any mat nor day light), (B) and (C) show the antibacterial result for Ag deposited on TiO_2/nylon-6 mat from a 1×10^{-4} M $AgNO_3$ solution for 60 s and a 2×10^{-4} M $AgNO_3$ solution for 120 s, respectively.

out without stirring the solution. Fig. 6 shows that the efficiency of free TiO_2 NPs and TiO_2 NPs in a polymer matrix is almost same, which confirms that the surface area of the TiO_2 NPs does not significantly decrease upon the incorporation of the NPs into the polymer fiber. Because our aim is to make a cost-effective photocatalyst, we performed an ability test of a reused Ag–TiO_2/nylon-6 mat for further photocatalytic reaction. For this purpose, a used fiber mat was kept in water for 7 days and reused after washing five times with distilled water. Then the photodegradation of MB was carried out under the same conditions as before. Fig. 6 shows that the efficiency of the reused mat is nearly similar to that of the initially used mat. We observed a slight decrease in the photocatalytic efficiency of the reused mat, which may be due to the deposition of byproduct particles on the surfaces of the NPs. Initially, the efficiency of the reused nanofibers was less than the initially used one, but after some time it was nearly equal, which indicates the presence of some foreign particles in the used mat. Moreover, the change in shape of the Ag NPs due to the intense solar radiation may be the cause of decreased photocatalytic efficiency.

Aeroxide (or Degussa) P25 TiO_2 forms a milky white turbid suspension in aqueous media, when it is used as photocatalyst. Furthermore, it does not settle quickly, which hinders its separation from the reaction mixture by centrifugation. The TiO_2 NPs that remain in natural water after the reaction (due to the recovery difficulty) are toxic to humans [3]. Therefore, the incorporation of these NPs into polymeric nanofibers can prevent this drawback. Our photocatalytic result shows that the reactivity of free TiO_2 NPs and TiO_2 NPs in the polymer matrix is almost same. Furthermore, it was observed that the Ag–TiO_2/nylon-6 mat can be reused many times as a photocatalyst because the efficiencies of the initially used and reused composite material are almost same (Fig. 6). This noble material may have great commercial potential as an economically friendly photocatalyst.

3.3. Antibacterial behaviors of the nanocomposite mats

The antimicrobial ability of the composite mats was tested by observing the survival of *E. coli* cells under daylight as described in Section 2.5. Fig. 7 shows the antibacterial efficiencies of the different composite mat surfaces against *E. coli* in daylight. To compare the results, a reference *E. coli* solution was kept in the dark. This dark and bacteria solution with nylon-6 or TiO_2/nylon-6 showed the same results as shown in Fig. 7(A). The results

showed that the Ag–TiO_2/nylon-6 nanocomposite mat has the lowest survivability of bacteria in day light (Fig. 7). It showed that the nylon-6 and TiO_2/nylon-6 mats did not show any antimicrobial effect, whereas the Ag–TiO_2/nylon-6 mat showed an antimicrobial effect. The actual mechanism of killing microorganisms with Ag in absence of UV light is not clear. Some researchers have proposed that Ag has innate antibacterial activity [33]. It is reported that Ag^+ hinders DNA replication and inhibits the expression of ribosomal proteins and enzymes for ATP hydrolysis [34,35]. It is believed that Ag nanoparticles display the same mechanism as Ag^+ and create a redox imbalance, which causes extensive bacterial death. It has been shown that the release of silver is controlled by an oxidation mechanism at the surface of the nanoparticles, which can prevent the loss of Ag NPs on the TiO_2 surface [36]. Furthermore, the antibacterial activity of Ag NPs on the surface of the TiO_2 NPs may be due to the plasmon resonance of the Ag NPs (at about 595 nm in our case). Here, photoexcited electrons may transfer from the surface of the Ag NPs to the conduction band of TiO_2. On the surface of the TiO_2 NPs, the injected electrons from Ag NPs are trapped by O_2 molecules and other species (e.g., $O_2^{\bullet -}$, $^{\bullet}OOH$, $^{\bullet}OH$) are generated [37]. The bacteria are oxidized by these species. To support this mechanism, we tested the photodeposition of Ag on a nanocomposite mat for longer time (120 s) with a more concentrated $AgNO_3$ solution (2×10^{-4} M). The efficiency of this mat was found to be greater than the mat that was obtained by the photodeposition of Ag from an $AgNO_3$ solution for 60 seconds with a concentration 1×10^{-4} M (Fig. 7). This result may be due to the increased quantity of transition of electrons from the increased number of Ag NPs to the conduction band of the TiO_2 NPs, where the electrons are used by O_2 molecules to generate large number of active species. As a result, we use TiO_2 as the anchoring sites for Ag NP deposition on the polymer surface. Furthermore, TiO_2 with polymer solution can give a spider-wave-like structure during electrospinning and therefore increase the surface area of the material, which can facilitate the deposition of Ag NPs on the well-dispersed TiO_2 NPs. The spider-wave-like structure becomes a good filter media, and the presence of TiO_2 NPs serves as antifouling agent [23], and the Ag NPs serve as an antimicrobial agent even in the absence of UV light. Therefore, this noble composite material can be used as a potential water filter media for people in developing countries, where access to modern water treatment technology is limited.

4. Conclusion

Ag–TiO_2/nylon-6 composite nanofiber mats were prepared via a combined technique involving electrospinning and photoreduction. TEM, XRD, EDX and UV–visible spectra analyses showed that the Ag NPs (approximately 4 nm in size) are homogeneously distributed throughout the TiO_2/nylon-6 spider-wave nanofibers and that they are selectively deposited on the surface of the TiO_2 without aggregation. The experimental results showed that the Ag–TiO_2/nylon-6 fiber nanocomposites have good photocatalytic and antimicrobial properties (even in absence of UV light), excellent recyclability and stability for potential applications in environmental remediation. The enhanced hydrophilicity (antifouling capacity) of the spider-wave-like structure of the nylon-6 composite mat due to the presence of TiO_2 NPs (reported in our previous work [23]) and the superior photocatalytic and antimicrobial properties of the deposited Ag NPs on the surface of the TiO_2 showed that the noble nanocomposite mat becomes an economically and environmentally friendly potential water filter media.

Acknowledgments

This research is supported by the Korean Research Foundation Grant funded by the Korean Government (MOEHRD) (Center for Healthcare Technology Development, Chonbuk National University, Jeonju 561-756, Republic of Korea). We thank Mr. Lee Young-Boo, KBSI, Jeonju branch, for taking the high-quality TEM images.

References

[1] A.L. Linsebigler, G.Q. Lu, J.T. Yates, Photocatalysis on TiO_2 surfaces: principles, mechanisms, and selected results, Chem. Rev. 95 (1995) 735–758.
[2] H. Schimidt, M. Naumann, T.S. Muller, M. Akarsu, Application of spray techniques for new photocatalytic gradient coatings on plastics, Thin Solid Films 502 (2006) 132–137.
[3] L. Reijenders, Hazard reduction for the application of titania nanoparticles in environmental technology, J. Hazard. Mater. 152 (2008) 440–445.
[4] A. Wold, Photocatalytic properties of titanium dioxide (TiO_2), Chem. Mater. 5 (1993) 280–283.
[5] M. Jakob, H. Levanon, P.V. Kamat, Charge distribution between UV-irradiated TiO_2 and gold nanoparticles. Determination of shift in Fermi level, Nano Lett. 3 (2003) 353–358.
[6] L. Shang, B. Li, W. Dong, B. Chen, C. Li, W. Tang, G. Wang, J. Wu, Y. Ying, Heteronanostructure of Ag particle on titanate nanowire membrane with enhanced photocatalytic properties and bactericidal activities, J. Hazard. Mater. 178 (2010) 1109–1114.
[7] B. Cheng, Y. Le, J. Yu, Preparation and enhanced photocatalytic activity of Ag@TiO_2 core–shell, J. Hazard. Mater. 177 (2010) 971–977.
[8] T. Matsunaga, R. Tomoda, T. Nakajima, H. Wake, Photo electrochemical sterilization of microbial cells by semi-conductor powders, FEMS Microbiol. Lett. 29 (1985) 211–214.
[9] J. Keleher, J. Bashant, N. Heldt, L. Johnson, Y. Li, Photo-catalytic preparation of silver-coated TiO_2 particles for antibacterial applications, World J. Microbiol. Biotechnol. 18 (2002) 133–139.
[10] K. Page, R.G. Palgrave, I.P. Parkin, M. Wilson, S.L.P. Savin, A.V. Chadwick, Titania and silver–titania composite films on glass—potent antimicrobial coatings, J. Mater. Chem. 17 (2007) 95–104.
[11] L. Sun, J. Li, C. Wang, S. Li, Y. Lai, H. Chen, C. Lin, Ultrasound aided photochemical synthesis of Ag loaded TiO_2 nanotube arrays to enhance photocatalytic activity, J. Hazard. Mater. 171 (2009) 1045–1050.
[12] D. Guin, S.V. Manorama, J.N.L. Latha, S. Singh, Photoreduction of silver on bare and colloidal TiO_2 nanoparticles/nanotubes: synthesis, characterization, and tested for antibacterial outcome, J. Phys. Chem. C 111 (2007) 13393–13397.
[13] J. Yu, J. Xiong, B. Cheng, S. Liu, Fabrication and characterization of Ag–TiO_2 multiphase nanocomposite thin films with enhanced photocatalytic activity, Appl. Catal. B: Environ. 60 (2005) 211–221.
[14] Y. Saito, J. Wang, D.N. Batchelder, D.A. Smith, Simple chemical method for forming silver surfaces with controlled grain sizes for surface plasmon experiments, Langmuir 19 (2003) 6857–6861.
[15] C. Guillard, H. Lachheb, A. Houas, M. Ksibi, E. Elaloui, J.M. Hermann, Influence of chemical structure of dyes, of pH and of inorganic salts on their photocatalytic degradation by TiO_2 comparison of the efficiency of powder and supported TiO_2, J. Photochem. Photobiol. A: Chem. 158 (2003) 27–36.
[16] H. Lachheb, E. Puzenat, A. Houas, M. Ksibi, E. Elaloui, C. Guillard, J.M. Hermann, Photocatalytic degradation of various types of dyes (Alizarin S, Crocein Orange G, Methyl Red, Congo Red, Methylene Blue) in water by UV-irradiated titania, Appl. Catal. B: Environ. 39 (2002) 75–90.
[17] M.S.A.S. Shah, M. Nag, T. Kalagara, S. Singh, S.V. Manorama, Silver on PEG–PU–TiO_2 polymer nanocomposite films: an excellent system for antibacterial applications, Chem. Mater. 20 (2008) 2455–2460.
[18] I.M. Arabatzis, T. Stergiopoulos, D. Andreeva, S. Kotova, S.G. Neophytides, P. Falaras, Characterization and photocatalytic activity of Au/TiO_2 thin films for azo-dye degradation, J. Catal. 220 (2003) 127–135.
[19] S.K. Lim, S.K. Lee, S.H. Hwang, H. Kim, Photocatalytic deposition of silver nanoparticles onto organic/inorganic composite nanofibers, Macro Matter Eng. 291 (2006) 1265–1270.
[20] T. Yuranova, R. Mosteo, J. Bandara, D. Laub, J. Kiwi, Self-cleaning cotton textiles surfaces modified by photoactive SiO_2/TiO_2 coating, J. Mol. Catal. A: Chem. 244 (2006) 160–167.
[21] T. Yuranova, A.G. Rincon, A. Bozzi, S. Parra, C. Pulgarin, P. Albers, J. Kiwi, Antibacterial textiles prepared by RF-plasma and vacuum-UV mediated deposition of silver, J. Photochem. Photobiol. A: Chem. 161 (2003) 27–34.
[22] H.R. Pant, M.P. Bajgai, K.T. Nam, Y.A. Seo, D.R. Pandeya, S.T. Hong, H.Y. Kim, Electrospun nylon-6 spider-net like nanofibers mat containing TiO_2 nanoparticles: a multifunctional nanocomposite textile material, J. Hazard. Mater. 185 (2010) 124–130.
[23] H.R. Pant, M.P. Bajgai, K.T. Nam, K.H. Chu, S.J. Park, H.Y. Kim, Formation of electrospun nylon-6/methoxy poly(ethylene glycol) oligomer spider-wave nanofibers, Mater. Lett. 64 (2010) 2087–2090.
[24] J.L. Pey, Corrosion protection of pipes, fitting and component pieces of water treatment and pumping stations, Anti-Corros. Methods Mater. 44 (1997) 94–99.
[25] J.S. Stephens, D.B. Chase, J.F. Rabolt, Effect of the electrospinning process on polymer crystallization chain conformation in nylon-6 and nylon-12, Macromolecules 37 (2004) 877–881.
[26] A.L. Linsebigler, G. Lu, J.T. Yates, Photocatalysis on TiO_2 surfaces: principles, mechanisms, and selected results, Chem. Rev. 95 (1995) 735–758.

[27] X. Wang, J.C. Yu, C. Ho, A.C. Mak, A robust three-dimensional mesoporous Ag/TiO_2 nanohybrid film, Chem. Commun. 17 (2005) 2262–2264.
[28] S. Jain, G. Dangi, J. Vardia, S.C. Ameta, Effects of the structure of TiO_2 nanotube array on Ti substrate on its photocatalytic activity, Int. J. Energy Res. 23 (1999) 71–77.
[29] C.Y. Wang, C.Y. Liu, X. Zheng, J. Chen, T. Shen, Effect of platinum on the photocatalytic decomposition of 2-chlorophenol in aqueous solution by UV/TiO_2, Colliod Surf. A 131 (1998) 271–280.
[30] V. Subramanian, E. Wolf, P. Kamat, To what extent metal nanoparticles (Au, Pt Ir) improve the photocatalytic activity of TiO_2 films, Phys. Chem. B 105 (2001) 11439–11446.
[31] W.S. Kuo, P.H. Ho, Solar photocatalytic decolorization of methylene blue in water, Chemosphere 45 (2001) 77–83.
[32] J.M. Herrmann, H. Tahiri, Y.A. Ichou, G. Lassaletta, A.R.G. Elipe, A. Fernandez, Characterization and photocatalytic activity in aqueous medium of TiO_2 and Ag–TiO_2 coatings on quartz, Appl. Catal. B 13 (1997) 219–228.
[33] V. Rupa, D. Manikandan, D. Divakar, T. Sivakumar, Effect of deposition of Ag on TiO_2 nanoparticles on the photodegradation of Reactive Yellow-17, J. Hazard. Mater. 147 (2007) 906–913.
[34] M. Yamanaka, K. Hara, J. Kudo, Bactericidal actions of a silver ion solution on *Escherichia coli*, studied by energy-filtering transmission electron microscopy and proteomic analysis, J. Appl. Environ. Microbiol. 71 (2005) 7589–7593.
[35] M.I. Mejia, G. Restrepo, J.M. Marin, R. Sanjines, C. Pulgarin, E. Mielczarski, J. Mielczarski, J. Kiwi, Magnetron-sputtered Ag surfaces. New evidence for the nature of the Ag ions intervening in bacterial inactivation, ACS Appl. Mater. Interf. 2 (2010) 230–235.
[36] D. Lee, R.E. Cohen, M.F. Rumner, Antibacterial properties of Ag nanoparticle loaded multilayers and formation of magnetically directed antibacterial microparticles, Langmuir 21 (2005) 9651–9659.
[37] H.M. Sung-Suh, J.R. Choi, H.J. Hah, S.M. Koo, Y.C. Bae, Comparison of Ah deposition effect on the photocatalytic activity of nanoparticulate TiO_2 under visible and UV light irradiation, J. Photochem. Photobiol. A 163 (2004) 37–44.